Catalysis Today 224 (2014) 34–40

Contents lists available at ScienceDirect

Catalysis Today

journal homepage: www.elsevier.com/locate/cattod

Simultaneous photocatalytic Cr(VI) reduction and 2,4,6-TCP oxidation over g-C_3N_4 under visible light irradiation

Xuefeng Hu[a,*], Huanhuan Ji[a], Fei Chang[b], Yongming Luo[a,*]

[a] Key Laboratory of Coastal Environmental Processes and Ecological Remediation, Yantai Institute of Coastal Zone Research, Chinese Academy of Sciences, Yantai, Shandong 264003, PR China
[b] School of Environment and Architecture, University of Shanghai for Science and Technology, Shanghai 200093, PR China

ARTICLE INFO

Article history:
Received 30 August 2013
Received in revised form 4 November 2013
Accepted 17 November 2013
Available online 8 December 2013

Keywords:
g-C_3N_4
Photocatalysis
2,4,6-TCP
Cr(VI) reduction, Visible light

ABSTRACT

In this study, a rapid reduction of Cr(VI) and degradation of 2,4,6-trichlorophenol (2,4,6-TCP) in a simultaneous manner was reported through the catalysis of g-C_3N_4 under visible light ($\lambda > 420$ nm) irradiation. The effects of initial concentration of reactants, dissolved O_2 and pH value were investigated systematically. It indicated that, under the optimized concentration, the Cr(VI) reduction and 2,4,6-TCP oxidation could be accomplished in couple of hours in the presence of g-C_3N_4. And also, the O_2 involvement and low pH value were able to significantly improve the removal rate of Cr(VI) and 2,4,6-TCP. In addition, the reaction mechanism was investigated through monitoring the reduced states of Cr(VI) and active oxygen intermediates formed during photoreaction by ESR and XPS, as well as determining the degradation products of 2,4,6-TCP by HPLC–MS. The results supported that the redox reactions of Cr(VI) and 2,4,6-TCP can be performed simultaneously via a synergistic oxidation–reduction mechanism in the presence of g-C_3N_4 under visible light irradiation.

1. Introduction

Semiconductor photocatalysis emerged as a promising technology for the purification of world environmental pollution [1–4]. Various toxic organic and inorganic pollutants could be transformed into harmless species after photoreaction. A major factor complicated the cleanup of polluted sites is the co-occurrence of organic compounds and heavy metals. However, most of researches on remediation technologies have focused on either organic compounds or metal ions, few can solve the pollutants from both the organic and metals. Semiconductor photocatalysis showed the potential in decontamination of the mixed pollutants because it is favorable for the reduction of metal ions and the oxidation of organic species.

2,4,6-TCP and chromium are common environmental pollutants, and classified as priority pollutants by the U.S. Environmental Protection Agency (EPA) [5–8]. The mixture of chlorophenol and chromium can be easily found in many waste streams, for instance tannery effluents. Chromium commonly presented as Cr(VI) and Cr(III) in nature. Cr(VI) is highly toxic and carcinogenic, while Cr(III) can be immobilized and thus become less bioavailable, so the reduction of Cr(VI) to Cr(III) is highly desired. Semiconductor photocatalyst, like TiO_2 could effectively reduce Cr(VI) to Cr(III) [9], and the reduction rate increased in the presence of organic compounds such as salicylic acid [10] and dye [11,12]. 2,4,6-TCP was decomposed to H_2O, CO_2 and Cl^- after photocatalytic reaction [13]. Fu et al. [14] and Sun et al. [15] reported that 4-chlorophenol (4-CP) and Cr(VI) could be simultaneously degraded and reduced by TiO_2 [14,15]. However, only less than 5% solar light can be used by TiO_2 because of its wide band gap (3.0 eV for the rutile phase and 3.2 eV for the anatase phase).

Recently, thermal polycondensation of common organic monomers was conveniently used to synthesize carbon nitride polymers close to the graphitic sheet-like structure (g-C_3N_4) [16]. Compared with TiO_2, g-C_3N_4 has an appropriate band gap (2.7 eV) for visible light absorption [17,18]. The capability of g-C_3N_4 in decomposing organic under visible light had attracted great attention, such as methyl orange (MO) [19], RhB [20], 4-CP [21]. Very recently, formate anion modified g-C_3N_4 was developed to photoreduce Cr(VI) [22], where the conduction band (CB) electrons were reported to govern the photoreaction of Cr(VI). Meanwhile, our previous work also demonstrated that the g-C_3N_4 was effective catalyst for 2,4,6-TCP oxidation and heavy metal (Cd^{2+}, Cu^{2+}, and Pb^{2+}) reduction [23]. However, the study for one-pot reduction of Cr(VI) and oxidation of 2,4,6-TCP has not been reported so far.

In this work, simultaneous reactions of Cr(VI) reduction and 2,4,6-TCP oxidation were studied systematically over bulk g-C_3N_4 under visible light irradiation. Control experiments were

* Corresponding authors. Tel.: +86 535 2109080; fax: +86 535 2109000.
E-mail addresses: xfhu@yic.ac.cn (X. Hu), ymluo@yic.ac.cn (Y. Luo).

0920-5861/$ – see front matter © 2013 Elsevier B.V. All rights reserved.
http://dx.doi.org/10.1016/j.cattod.2013.11.038

performed to reveal the role of Cr(VI), 2,4,6-TCP and g-C_3N_4 on the oxidation and reduction processes. The effects of initial concentration, pH, and dissolved oxygen were also studied. A synergistic reduction–oxidation mechanism was finally proposed base on the experimental results.

2. Experimental

2.1. Reagents and solutions

Dicyandiamide (>98.0%) was purchased from Tokyo Chemical Industry Co., Ltd. (Tokyo, Japan). 2,4,6-Trichlorophenol (2,4,6-TCP) (98%) was purchased from Aladdin Chemistry Co., Ltd. (Shanghai, China). $K_2Cr_2O_7$ (>99.8%) was purchased from Tianjin Tianda Chemical Experiment Factory (Tianjin China). All reagents were used as received without further purification. Freshly deionized water (18.2 MΩ cm specific resistance) generated by a Pall Cascada laboratory water system was used to prepare all solutions. 2,4,6-TCP (10^{-3} M) and Cr(VI) (10^{-2} M) stock solutions were prepared by dissolving 2,4,6-TCP (98%) or $K_2Cr_2O_7$ (A.R.) into deionized water.

2.2. Material preparation and characterization

In this study, g-C_3N_4 catalyst was prepared using thermal condensation of dicyandiamide method [24] and strictly according to our previous report [23]. A 50 mL ceramic crucible containing 2 g dicyandiamide was introduced into a muffle furnace. Within 4 h, the temperature of the furnace raised to 550 °C from room temperature in air conditions and kept at this temperature for 4 h. The obtained yellow product was collected and ground into powder prior to use.

The crystal structure of the sample was investigated using X-ray diffraction (XRD; Rigaka D/max 2500 X-ray diffractometer) with Cu Kα_1 radiation, λ = 1.54056 Å. X-ray photoelectron spectroscopy (XPS) data were obtained with an ESCALab220i-XL electron spectrometer from VG Scientific using 300 W Al Kα radiation. The binding energies were referenced to the C1s line at 284.8 eV from adventitious carbon. Elemental analysis (EA) was carried out on an Elemental Vario III elemental analyzer. The Fourier transform infrared (FT-IR) spectrum of the sample was recorded on a Nicolet iS 10 FT-IR spectrometer. The electron spin resonance (ESR) technique was used to detect Cr transients and hydroxyl radicals on a Bruker (ESP 300E) spectrometer equipped with a 532 nm laser. Before hydroxyl radicals measurement, DMPO was added to the catalyst aqueous suspension. The EPR settings were modulation amplitude 1.94 G and microwave frequency 9.750 GHz.

2.3. Photocatalytic experiments

Cr(VI)/2,4,6-TCP reaction solution was prepared by diluting certain volume of 2,4,6-TCP and Cr(VI) stock solution to 30 mL with deionized water in a 50 mL serum bottle. The finally concentration of Cr(VI) and 2,4,6-TCP were respectively 2×10^{-4} M and 1×10^{-4} M unless otherwise noted. Before irradiation, 30 mg g-C_3N_4 was added to the solution and magnetically stirred for 0.5 h in dark to obtain adsorption/desorption equilibrium. The light irradiation system was equipped with a 300 W Xe lamp (CEL-HXF300, Beijing Aulight Co., Ltd.) and a cut-off filter to ensure the wavelength of irradiation light is above 420 nm. The light intensity impinging on the suspension was 150 mW/cm^2 as measured with a radiometer (CEL-NP2000, Beijing Aulight Co., Ltd.). During photoreaction, 3 mL aliquots were sampled at every 0.5 h interval for subsequent analysis after centrifugation and filtration.

2.4. Analysis

The concentration of 2,4,6-TCP was measured by a HPLC (waters 2695–2998) system. LC–MS information was given by coupling HPLC with a LCQ Fleet ion-trap mass spectrometer (Thermo Fisher Scientific, USA) installed with a Xcalibur software. The diphenylcarbazide photometric method (Chinese National Standard Procedure, GB7467-87) was used to analyze Cr(VI) concentration at 540 nm by a spectrophotometer (Beckman coulter DU800). Standard curve was plotted (Fig. S1) and the Cr(VI) concentration was estimated based on the standard curve. For total Cr examination, $KMnO_4$ was used to oxidize lower valent Cr to Cr(VI). For H_2O_2 concentration analysis, 1 mL sample, 1 mL pH 6.0 buffer, 50 μL DPD and 50 μL POD were mixed in a 1 cm cuvette. The absorption spectrum of DPD oxidation product (DPD^+) at 550 nm was measured after 45 s reaction by a spectrophotometer (Beckman coulter DU800). However, the determination of H_2O_2 was disturbed due to Cr(VI) can oxidize DPD directly. For this reason, the absorption of DPD^+ in the absence of POD was measured as a background to eliminate the disturbance of Cr(VI). Preparation of pH buffer, DPD and POD solution, as well as the calculation of H_2O_2 concentration were performed according to literature [25]. The released chloride ions were monitored using an ion chromatograph (Dionex ICS3000). The buffer solution was 4.5 mM Na_2CO_3/0.8 mM $NaHCO_3$, and a Dionex AS18 column was used.

3. Results and discussion

3.1. Structural features of the g-C_3N_4

The XRD pattern (Fig. S2) of the as-prepared g-C_3N_4 are dominated by the characteristic (0 0 2) peak at 27.42 of a interlayer stacking peak of aromatic systems. The relatively weak peak at 13.14, which is indexed as (1 0 0) plane, is associated with an in-plane structural packing motif. The elemental analysis of the catalyst provided an average C/N molar ratio value of 0.67 (theoretical value:0.75 for C_3N_4). The additional small amount of hydrogen we found (2.3%) were attributed to the uncondensed amino functions, adsorbed water and structural defects on the surface [26].

The Fourier transform infrared (FT-IR) result proves that the existence of a graphite-like structure of carbon nitride again as shown in Fig. S3. Several strong bands in the 1200–1650 cm^{-1} region correspond to the typical stretching modes of CN heterocycles. Additionally, the characteristic ring breath of the triazine units is found at 809 cm^{-1} [23].

3.2. Synergistic effect of Cr(VI) reduction and 2,4,6-TCP degradation over g-C_3N_4

The feasibility of photocatalytic decontamination of the mixture containing Cr(VI) and 2,4,6-TCP over g-C_3N_4 was investigated firstly. As illustrated in Fig. 1A and B, 2×10^{-4} M Cr(VI) was completely reduced over g-C_3N_4 after 3 h visible light irradiation. Meanwhile, 10^{-4} M 2,4,6-TCP co-existed in the reaction system was also consumed after 2 h irradiation. Simultaneous photoreduction of Cr(VI) and photodegradation of 2,4,6-TCP were achieved successfully.

To make clear the role of each substrate, control experiments were conducted. The reduction of Cr(VI) is negligible in the absence of 2,4,6-TCP or g-C_3N_4, as shown in Fig. 1A. Similarly, the very low reaction rate between Cr(VI) and chlorophenol under visible light irradiation was also reported [15]. It is general that g-C_3N_4 can created electrons and holes under visible light, and the generated electrons can be used for the reduction of Cr(VI). However, the photogenerated holes of g-C_3N_4 are incapable of oxidizing the

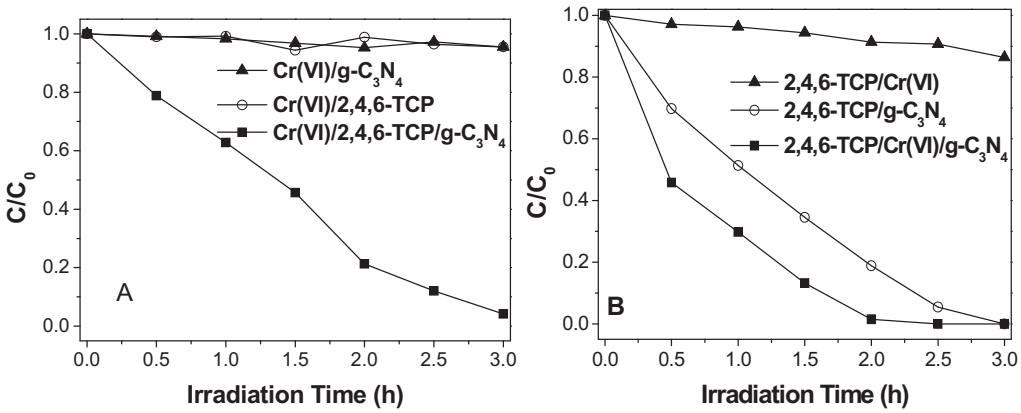

Fig. 1. The synergistic effect of Cr(VI) reduction and 2,4,6-TCP degradation over g-C_3N_4 under visible light irradiation: (A) Cr(VI) reduction and (B) 2,4,6-TCP degradation.

surface hydroxyl groups directly because of its low oxidation potential (1.53 V) [27]. It is difficult to achieve effective electron–hole pairs separation and then reduce Cr(VI) in the absence of electron donor, 2,4,6-TCP. As seen from Fig. 1B, only approximately 15% 2,4,6-TCP was degraded within three hours in the 2,4,6-TCP/Cr(VI) system, which is consistent with the low reduction rate of Cr(VI) in Fig. 1A. g-C_3N_4 could degrade 2,4,6-TCP alone, but it took total 3 h to remove 2,4,6-TCP (10^{-4} M) completely in the 2,4,6-TCP/g-C_3N_4 system. However, in the 2,4,6-TCP/Cr(VI)/g-C_3N_4 system, the complete removal of 2,4,6-TCP (10^{-4} M) was accomplished merely after 2 h. These results confirmed the synergistic effect of Cr(VI) reduction and 2,4,6-TCP oxidation.

3.3. Effect of TCP and Cr(VI) concentration

As discussed above, 2,4,6-TCP and Cr(VI) enhanced each other's removal in the g-C_3N_4 photocatalytic reaction system. Various 2,4,6-TCP and Cr(VI) initial concentrations were used to further investigate their interaction during photoreaction. 2,4,6-TCP, as an electron donor, react irreversibly with the photogenerated VB holes can enhance the photocatalytic electron–hole separation, which results in much more CB electrons for Cr(VI) reduction. As shown in Fig. 2A, low concentration (5×10^{-5}) of 2,4,6-TCP cannot capture the VB holes efficiently and then the reduction rate of Cr(VI) was low. 10^{-4} M 2,4,6-TCP is optimal for 2×10^{-4} M Cr(VI) reduction in our reaction condition. However, further increase of the 2,4,6-TCP concentration suppressed Cr(VI) reduction. Fig. 2B shows 2,4,6-TCP degradation rates increased along with the initial concentration of Cr(VI) from 0 to 5×10^{-4} M. There was no appreciable increase of 2,4,6-TCP degradation rate with further increasing the Cr(VI) concentration to 10^{-3} M.

3.4. Effect of pH

In this section, the effect of solution pH was investigated and the results were plotted in Fig. 3. Compared to the alkaline and neutral conditions, Cr(VI) reduction and 2,4,6-TCP degradation both take place much quickly in acid conditions. Generally, the reaction rates increased with the decrease of pH value, especially for the Cr(VI) reduction. Under neutral and alkaline conditions, the Cr(VI) reduction is negligible, and the 2,4,6-TCP degradations were very slow. The results may be caused by the following three reasons. (1) The reduction potential of Cr(VI)/Cr(III) shift 138 mV per pH unit to more cathodic potentials, whereas the conduction band of the semiconductor shifts 59 mV per pH [28]. Consequently, the thermodynamic driving force for the reduction of Cr(VI) decreased by 79 mV with an increase of pH by one unit. (2) From the simulation of the Cr(VI) speciation with Visual MINTEQ, $HCrO_4^-$ was the major Cr(VI) species below pH 5, while CrO_4^{2-} was the major species above pH 7. This results suggested that the reduction of Cr(VI) could be described by Eq. (1) when the pH value is below 5, while its reduction could be described by Eq. (2) when the pH value is above 7. The increasing reaction rate with an increase in acidity was interpreted in terms of higher susceptibility of $HCrO_4$ than CrO_4^{2-} to undergo reduction [29]. (3) In the neutral and alkaline conditions, Cr(III) could precipitate on the surface of g-C_3N_4 in the form of $Cr(OH)_3$, suppressing the activity of catalyst.

$$HCrO_4^- + 7H^+ + 3e^- \rightarrow Cr^{3+} + 4H_2O \quad (1)$$

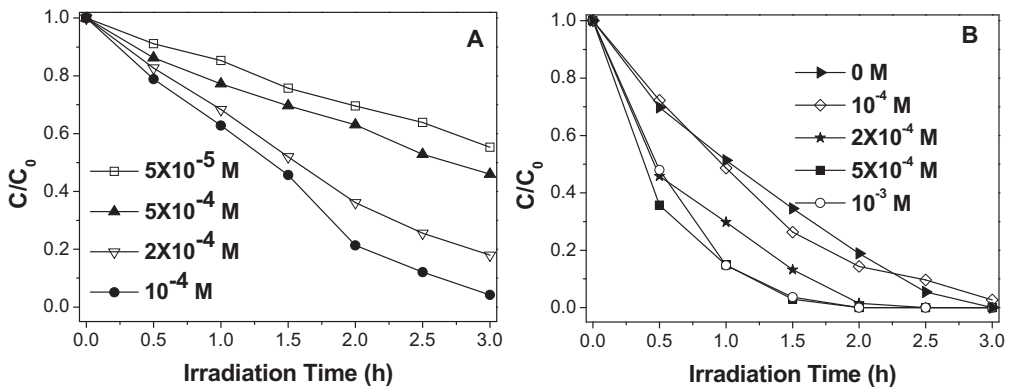

Fig. 2. The effects of (A) 2,4,6-TCP initial concentration on Cr(VI) (2×10^{-4} M) reduction and (B) Cr(VI) initial concentration on 2,4,6-TCP (1×10^{-4} M) degradation.

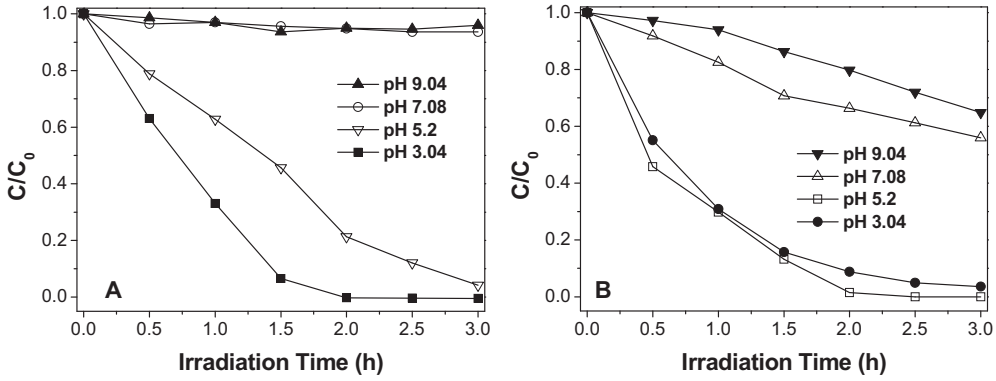

Fig. 3. (A) Cr(VI) reduction and (B) 2,4,6-TCP degradation at different pH condition in the 2,4,6-TCP/Cr(VI)/g-C_3N_4 reaction system.

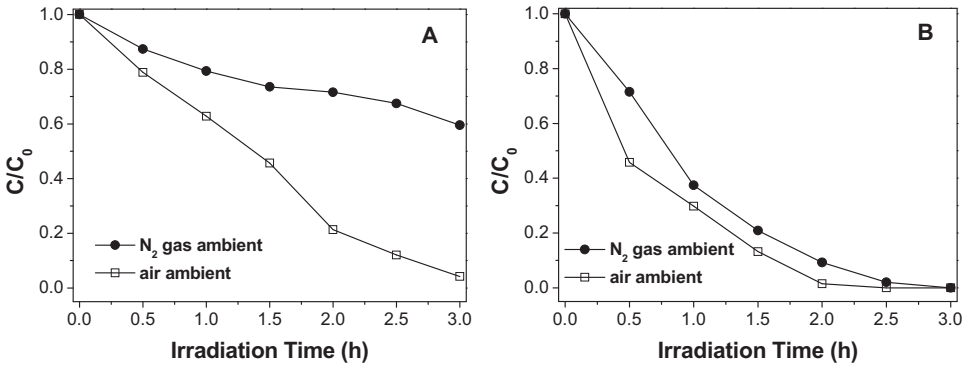

Fig. 4. (A) Cr(VI) reduction and (B) 2,4,6-TCP degradation at different ambient in the 2,4,6-TCP/Cr(VI)/g-C_3N_4 reaction system.

$$CrO_4^{2-} + 8H^+ + 3e^- \rightarrow Cr^{3+} + 4H_2O \quad (2)$$

3.5. Effect of dissolved oxygen

Fig. 4 shows that Cr(VI) reduction and 2,4,6-TCP degradation were both suppressed in N_2 ambient. The suppression effect was more evident for Cr(VI) reduction, it is just ca. 40% Cr(VI) was reduced in N_2 gas ambient compared with 100% reduction in air after 3 h photoreaction. The phenomenon illustrated that O_2 played an important role in the photocatalytic reaction. In aerated systems, the conduction band electrons, formed by photoexcition of catalyst, are usually scavenged by O_2 to yield superoxide radical $O_2^{\bullet-}$/$^{\bullet}$OOH (Eqs. (3) and (4)) or by other electron acceptor [2]. $O_2^{\bullet-}$ and its further reduction/disproportionation products (H_2O_2, $^{\bullet}$OH) (Eqs. (5)–(7)) are important active oxidative species in the degradation of organic pollutants [30]. It had been reported that $O_2^{\bullet-}$ react with Cr(VI) to generate Cr(V) (Eq. (8)) [31]. Then $O_2^{\bullet-}$ may also contribute to the Cr(VI) reduction during photoreaction. For these reasons, the rate of 2,4,6-TCP degradation and Cr(VI) reduction is higher in air than that in N_2 atmosphere.

$$O_2 + e^- \rightarrow O_2^{\bullet-} \quad (3)$$

$$O_2^{\bullet-} + H^+ \rightarrow {}^{\bullet}OOH \quad (4)$$

$$2O_2^{\bullet-} + 2H^+ \rightarrow O_2 + H_2O_2 \quad (5)$$

$$O_2^{\bullet-} + e^- + 2H^+ \rightarrow H_2O_2 \quad (6)$$

$$H_2O_2 + e^- \rightarrow {}^{\bullet}OH + OH^- \quad (7)$$

$$O_2^{\bullet-} + Cr(VI) \rightarrow Cr(V) + O_2 \quad (8)$$

3.6. Pathways of Cr(VI) reduction

Reduction of Cr(VI) to Cr(III) was a global three-electron-transfer reaction. It had been reported that Cr(VI) reduction occurred via sequential one-electron-transfer steps (Eq. (9)) in a TiO_2 photocatalyzed system [32]. Whether Cr(VI) was reduced through one-electron-transfer steps or by reacting with $O_2^{\bullet-}$, Cr(V) was the intermediate. ESR spectroscopy is deemed as a powerful tool for studying Cr(V) transients generated during the reduction of Cr(VI). From the ESR spectra in Fig. 5, a *g* value of 1.9527 was determined, which is assigned to Cr(V) [32].

$$Cr(VI) \xrightarrow{e^-} Cr(V) \xrightarrow{e^-} Cr(IV) \xrightarrow{e^-} Cr(III) \quad (9)$$

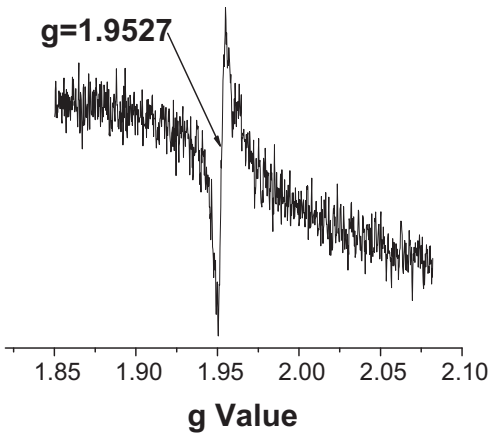

Fig. 5. EPR spectra of Cr(V) formed under visible irradiation of TCP/Cr(VI)/g-C_3N_4 reaction system.

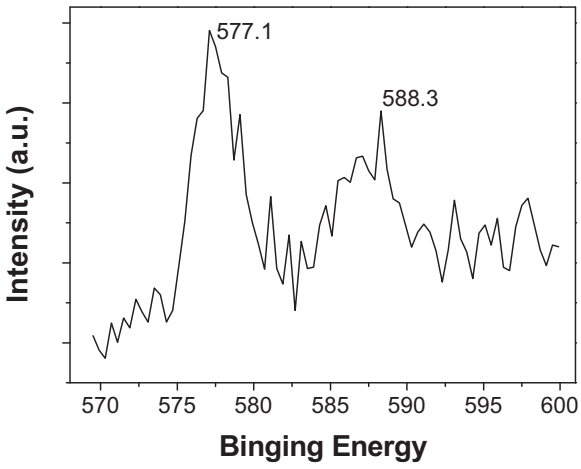

Fig. 6. Cr 2p spectrum of chromium on g-C_3N_4 after photoreaction.

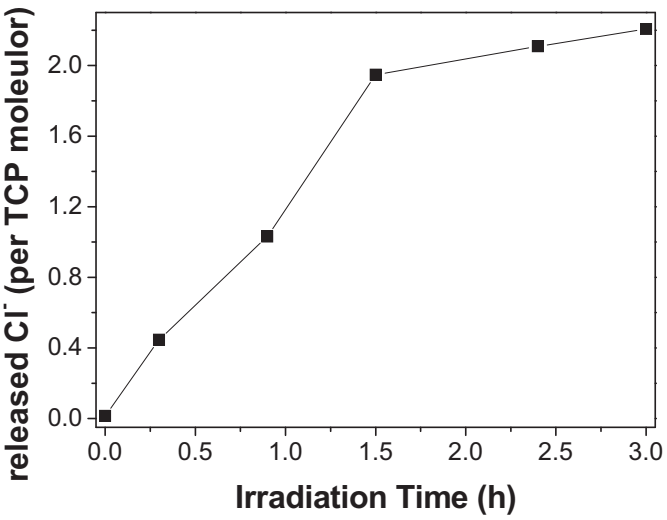

Fig. 8. Chloride ions release during 2,4,6-TCP degradation in the 2,4,6-TCP/Cr(VI)/g-C_3N_4 system under visible light irradiation.

Both the reduction of Cr(VI) by photogenerated CB electrons of g-C_3N_4 directly and by $O_2^{\bullet-}$ (Eq. (9)) [33] are possible reaction mechanism in the present photoreaction system. The increased reduction rate of Cr(VI) in the presence of O_2 confirming the important roles of $O_2^{\bullet-}$. However, Cr(VI) can be reduced in the absence of O_2 as seen in Fig. 4A. This indicated that CB electrons of g-C_3N_4 were also contributed to the reduction of Cr(VI). Together with the Cr(VI) reduction experiments in the presence and absence of oxygen, both of the above two pathways should take responsibility for Cr(VI) reduction.

Fu et al. [14] reported that when 4-chlorophenol was subjected to UV irradiation and then Cr(VI) was added and placed in darkness, the reduction reaction of Cr(VI) was still in progress. Then, the dark thermal reaction between Cr(VI) and photodegradation products of 2,4,6-TCP is another possible pathway of Cr(VI) reduction. However, the reduction of Cr(VI) stopped immediately after ceasing visible light irradiation in the 2,4,6-TCP/Cr(VI)/g-C_3N_4 system (this result was not shown). So, the reduction of Cr(VI) by degradation products of 2,4,6-TCP was not supported in this reaction system.

On the basis of the above analysis, it can be concluded that Cr(VI) is reduced via two pathways: (1) by photogenerated CB electrons of g-C_3N_4 directly and (2) by $O_2^{\bullet-}$ indirectly.

3.7. Adsorption of chromium on g-C_3N_4

XPS was used to determine the Cr adsorbed on g-C_3N_4 before and after photoreaction. We cannot observe the signal of chromium on g-C_3N_4 even after 24 h adsorption of Cr(VI) on g-C_3N_4 in dark (Fig. S4). However, the chromium signal occurred after 3 h photoreaction, the spectrum of XPS of resultant product was shown in Fig. 6. The banding energy of Cr $2p_{2/3}$ of Cr(VI) are ca. 579 eV, while the banding energy of Cr $2p_{2/3}$ of Cr(III) are usually around 577 eV [30]. The 577.1 eV signal of Cr $2p_{2/3}$ in the present experiment is closed to Cr(III). Together with the phenomenon that Cr $2p_{2/3}$ signals observed only after photoreaction, we think that the XPS signals came mainly from Cr(III). The result suggested that Cr(VI) was reduced during photoreaction and the resultant Cr(III) adsorbed on the surface of catalyst. The ζ-potential of g-C_3N_4 was −18.6 mV as measured [31], so the negative charged surface of g-C_3N_4 would prefer to adsorb positively charged Cr(III) rather than negatively charged Cr(VI).

The adsorption of chromium on g-C_3N_4 was also investigated by measuring Cr(VI) and total chromium in solution. Adsorption of Cr(VI) on g-C_3N_4 before photoreaction was examined in dark. Adsorption/desorption equilibrium between the catalyst and Cr(VI) was established after 0.5 h stir, ca. 4% Cr(VI) was adsorbed on g-C_3N_4. At the initial photoreaction stage, the total Cr decrease was closed to that of Cr(VI), but the removal of total Cr was slower than that of Cr(VI) after one hour reaction. Since the reaction was performed in acidic condition (pH about 5.0), the formation of $Cr(OH)_3$ precipitation is neglected. So it is supposed, Cr(III) ions were almost adsorbed onto g-C_3N_4 surface when Cr(VI) was reduced at the first stage. Along with the reaction, part of the adsorption sites were occupied and then the adsorption of Cr(III) became difficult. Over 50% total chromium was removed from the solution when Cr(VI) was completely reduced after 3 h.

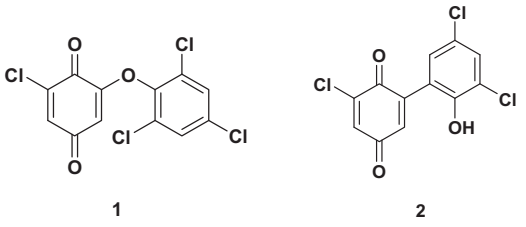

Fig. 7. Structures of the identified coupling products in the 2,4,6-TCP/Cr(VI)/g-C_3N_4 complex system after 0.5 h photoreaction.

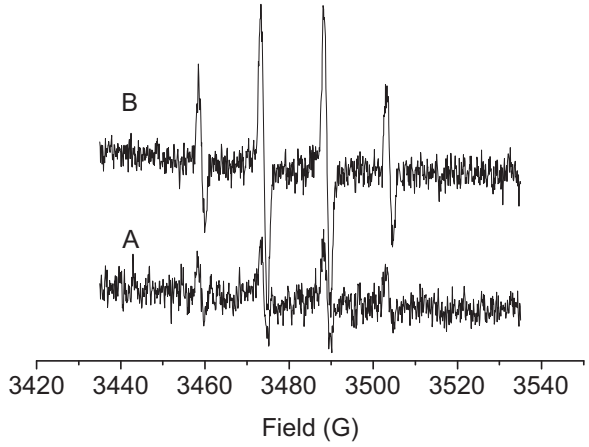

Fig. 9. ESR spectra of DMPO-·OH adducts formed by C_3N_4 after 80 s visible light irradiation (532 nm) in the absence (A) and presence (B) of Cr (VI).

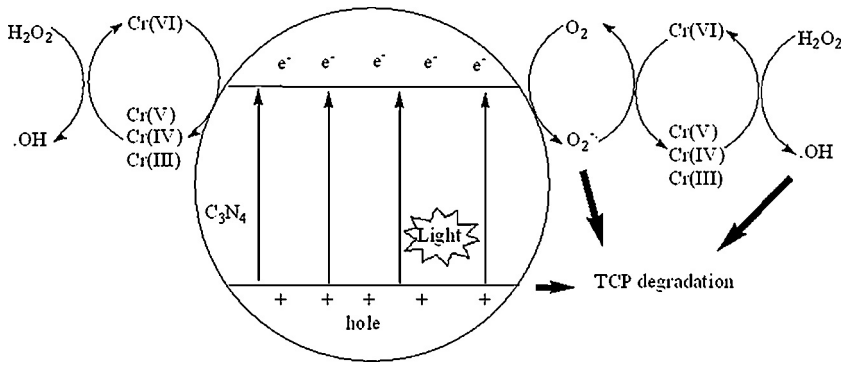

Fig. 10. Reaction pathway of Cr(VI) reduction and 2,4,6-TCP degradation over g-C_3N_4 under visible light irradiation.

3.8. Degradation intermediates and Cl^- release of 2,4,6-TCP

Four intermediates including 2,6-dichloro-3-hydroxy-1,4-benzoquinone (DCHB), 2,6-dichloro-1,4-benzoquinone (2,6-DCQ), 4,6-dichloro-catechol (4,6-DCC) and 2,3,4,6-tetrachlorophenol (TRCP) were found in the 2,4,6-TCP/g-C_3N_4 photocatalytic system as seen in our previous report [23]. Apart from these four intermediates, other new high m/z peaks were also observed in the 2,4,6-TCP/Cr(VI)/g-C_3N_4 system after 0.5 h photoreaction. Two of them were identified as shown in Fig. 7: (1) m/z 335 $[M-H]^-$, (2) m/z 301 [M−H] based on their isotope peaks and literature [34]. Other unidentified products may also result from the coupling of degradation intermediates of 2,4,6-TCP, but their structures have not been elucidated yet.

The release of chloride ion was used to evaluate the overall efficiency of 2,4,6-TCP photodegradation. As shown in Fig. 8, concentration of chloride ions increased as the function of irradiation time in the reaction solution. When the reaction finished in 3 h, about 2.2 chloride ions per 2,4,6-TCP molecule were released into the reaction solution.

The distinct color change in reaction solution along with the irradiation time was observed (Fig. S5). The original color of 2,4,6-TCP solution is colorless while the color of the Cr(VI) and 2,4,6-TCP solution was faint yellow coming from Cr(VI). The Cr(VI) and 2,4,6-TCP solution then changed to pink color after 1 h photoreaction under visible light irradiation in the presence of g-C_3N_4. The pink color should come from the intermediate DCHB as we reported before [35]. Along with reaction, the color disappeared gradually, and the solution becomes colorless after 3 h. The color changes also illustrated that Cr(VI) reduction and 2,4,6-TCP degradation were achieved simultaneously in the present photoreaction system.

3.9. Photoreaction mechanism

Based on the above discussion, the reduction of Cr(VI) could be achieved via direct electron transfer from CB of g-C_3N_4, or by reaction of $O_2^{\bullet-}$ with Cr(VI). In details, upon g-C_3N_4 excitation, the electron transferred to the conduction band first, and then captured by oxygen to form $O_2^{\bullet-}$ or by Cr(VI) to form lower valence states chromium. The negatively charged surface of g-C_3N_4 would prefer to adsorb neutral molecular oxygen rather than negatively charged $HCrO_4^-$, then $O_2^{\bullet-}$ govern the reduction of Cr(VI). High concentration of 2,4,6-TCP would compete adsorption sites and $O_2^{\bullet-}$ with Cr(VI). It is reasonable that Cr(VI) reduction was suppressed when 2,4,6-TCP concentration higher than 10^{-4} M as mentioned above.

On one hand, $O_2^{\bullet-}$ can converse to another oxidant H_2O_2 (Eqs. (5) and (6)), and about 38 μM of H_2O_2 was detected in g-C_3N_4/2,4,6-TCP after 3 h visible light irradiation [23]. However, the generation of H_2O_2 was only 2 μM in g-C_3N_4/2,4,6-TCP/Cr(VI) under the same irradiation condition. This implies that H_2O_2 should be consumed as soon as it is generated in the ternary system. It has been reported that the lower valence states of chromium can react with H_2O_2 to form hydroxyl radicals (Eqs. (10)–(12)) [36,37]. ESR experiments showed that the DMPO-·OH adducts signal was stronger in the presence of Cr(VI) than its absence after 80 s visible light irradiation over g-C_3N_4, Fig. 9. The formation of hydroxyl radicals in the presence of Cr(VI) may be responsible for the enhanced degradation rate of 2,4,6-TCP. On the other hand, $O_2^{\bullet-}$ are also contribute to the degradation of 2,4,6-TCP directly [23]. The photodegradation of 2,4,6-TCP in N_2 gas ambient well illustrated that 2,4,6-TCP could be degraded by VB holes when photogenerated electrons were scavenged by Cr(VI). Increase of the Cr(VI) concentration would facilitate the trapping of CB electrons and effectively promote the electron–hole separation, therefore enhance the degradation rate of 2,4,6-TCP as shown in Fig. 1B. Compared to 2,4,6-TCP/g-C_3N_4 single system, Cr(VI)/2,4,6-TCP/g-C_3N_4 complex system facilitate the formation of coupling products. From the above analysis, both the active oxygen species ($O_2^{\bullet-}$ and $^{\bullet}OH$) and hole are responsible for the degradation of 2,4,6-TCP in the Cr(VI)/2,4,6-TCP/g-C_3N_4 photoreaction system.

$$H_2O_2 + Cr(V) \rightarrow {}^{\bullet}OH + OH^- + Cr(VI) \quad (10)$$

$$H_2O_2 + Cr(IV) \rightarrow {}^{\bullet}OH + OH^- + Cr(V) \quad (11)$$

$$H_2O_2 + Cr(III) \rightarrow {}^{\bullet}OH + OH^- + Cr(IV) \quad (12)$$

The overall reaction pathway of Cr(VI) reduction and 2,4,6-TCP degradation over g-C_3N_4 under visible light was shown in Fig. 10.

4. Conclusion

The synergistic effect of Cr(VI) reduction and 2,4,6-TCP degradation was observed over g-C_3N_4 under visible light irradiation. Various conditions were performed to optimize the synergistic effect and investigate the reaction mechanism. The results indicated that acidic environment was beneficial for the reduction of Cr(VI) and oxidation of 2,4,6-TCP. The presence of oxygen could improve the reaction rate for both Cr(VI) reduction and 2,4,6-TCP oxidation. The initial concentration of substrates will affect the reaction rate in a certain concentration range. Mechanistically understanding, both CB electrons and $O_2^{\bullet-}$ responsible for the reduction of Cr(VI), and most the reduced Cr(III) was adsorbed on the g-C_3N_4 surface. Coupling products was generated in the presence of Cr(VI) during 2,4,6-TCP photodegradation. There are still some Cl-containing intermediates exist in the solution after 2,4,6-TCP degrade completely. We should take care the potential risk of the Cl-containing intermediates. Hole of VB, $O_2^{\bullet-}$ and ·OH derived from the reaction between reduced states of chromium and H_2O_2 enhanced the degradation rate of 2,4,6-TCP.

Acknowledgments

The generous supports by the National Natural Science Foundation of China (Nos. 41076040, 41230858 and 21207089) are acknowledged.

Appendix A. Supplementary data

Supplementary data associated with this article can be found, in the online version, at http://dx.doi.org/10.1016/j.cattod.2013.11.038.

References

[1] A. Mills, R.H. Davies, D. Worsley, Chem. Soc. Rev. 22 (1993) 417–425.
[2] M.R. Hoffmann, S.T. Martin, W. Choi, D.W. Bahnemann, Chem. Rev. 95 (1995) 69–96.
[3] W. Choi, Catal. Surv. Asia 10 (2006) 16–28.
[4] X.F. Chen, X.C. Wang, X.Z. Fu, Energy Environ. Sci. 2 (2009) 872–877.
[5] R. Andreozzi, I.D. Somma, R. Marotta, G. Pinto, A. Pollio, D. Spasiano, Water Res. 45 (2011) 2028–2048.
[6] G.L. Saylor, L. Chen, M.J. Kupferle, Environ. Toxicol. Chem. 31 (2012) 494–500.
[7] Y.C. Sharma, C.H. Weng, J. Hazard. Mater. 142 (2007) 449–454.
[8] Y.T. Wang, H. Shen, J. Ind. Microbiol. 14 (1995) 159–163.
[9] C.R. Chenthamarakshan, K. Rajeshwar, E.J. Wolfrum, Langmuir 16 (2000) 2715–2721.
[10] G. Colón, M.C. Hidalgo, J.A. Navío, J. Photochem. Photobiol. A: Chem. 138 (2001) 79–85.
[11] S.G. Schrank, H.J. José, R.F.P.M. Moreira, J. Photochem. Photobiol. A: Chem. 147 (2002) 71–76.
[12] M.V. Dozzi, A. Saccomanni, E. Selli, J. Hazard. Mater. 211–212 (2012) 188–195.
[13] E. Androulaki, A. Hiskia, D. Dimotikali, C. Minero, P. Calza, E. Pelizzetti, E. Papaconstantinou, Environ. Sci. Technol. 34 (2000) 2024–2028.
[14] H. Fu, G. Lu, S. Li, J. Photochem. Photobiol. A: Chem. 114 (1998) 81–88.
[15] B. Sun, E.P. Reddy, P.G. Smirniotis, Environ. Sci. Technol. 39 (2005) 6251–6259.
[16] J.S. Zhang, X.D. Chen, K. Takanabe, K. Maeda, K. Domen, J.D. Epping, X.Z. Fu, M. Antonietti, X.C. Wang, Angew. Chem. Int. Ed. 49 (2010) 441–444.
[17] X.C. Wang, K. Maeda, X.F. Chen, K. Takanabe, K. Domen, Y.D. Hou, X.Z. Fu, M. Antonietti, J. Am. Chem. Soc. 131 (2009) 1680–1681.
[18] Y. Wang, X.C. Wang, M. Antonietti, Angew. Chem. Int. Ed. 51 (2012) 68–89.
[19] S.C. Yan, Z.S. Li, Z.G. Zou, Langmuir 25 (2009) 10397–10401.
[20] Y.J. Cui, Z.X. Ding, P. Liu, M. Antonietti, X.Z. Fu, X.C. Wang, Phys. Chem. Chem. Phys. 14 (2012) 1455–1462.
[21] Y.J. Cui, J.H. Huang, X.Z. Fu, X.C. Wang, Catal. Sci. Technol. 2 (2012) 1396–1402.
[22] G.H. Dong, L.Z. Zhang, J. Phys. Chem. C 117 (2013) 4062–4068.
[23] H.H. Ji, F. Chang, X.F. Hu, W. Qin, J.W. Shen, Chem. Eng. J. 218 (2013) 183–190.
[24] X.C. Wang, K. Maeda, A. Thomas, K. Takanabe, G. Xin, J.M. Carlsson, K. Domen, M. Antomietti, Nat. Mater. 8 (2009) 76–80.
[25] H. Bader, V. Sturzenegger, J. Hoigné, Water Res. 22 (1988) 1109–1115.
[26] F. Goettmann, A. Fischer, M. Antonietti, A. Thomas, Chem. Commun. (2006) 4530–4532.
[27] S.C. Yan, Z.S. Li, Z.G. Zou, Langmuir 26 (2010) 3894–3901.
[28] X.L. Wang, S.O. Pehkonen, A.K. Ray, Ind. Eng. Chem. Res. 43 (2004) 1665–1672.
[29] P. Mytych, A. Karocki, Z. Stasicka, J. Photochem. Photobiol. A: Chem. 160 (2003) 163–170.
[30] C.C. Chen, W.H. Ma, J.C. Zhao, Chem. Soc. Rev. 39 (2010) 4206–4219.
[31] S.W. Wang, S.S. Leonard, J.P. Ye, N. Gao, L.Y. Wang, X.L. Shi, Mol. Cell. Biochem. 255 (2004) 119–127.
[32] J.J. Testa, M.A. Grela, M.I. Litter, Langmuir 17 (2001) 3155–3157.
[33] X.L. Shi, A. Chiu, C.T. Chen, B. Halliwell, V. Castranova, V. Vallyathan, J. Toxicol. Environ. Health B: Crit. Rev. 2 (1999) 87–104.
[34] G. Díaz-Díaz, M. Celis-García, M.C. Blanco-López, M.J. Lobo-Castañón, A.J. Miranda-Ordieres, P. Tuñón-Blanco, Appl. Catal. B 96 (2010) 51–56.
[35] X.F. Hu, H.H. Ji, L. Wu, RSC Adv. 2 (2012) 12378–12383.
[36] H. Luo, Y.D. Lu, Y. Mao, X.L. Shi, N.S. Dalar, J. Inorg. Biochem. 64 (1996) 25–35.
[37] T.C. Tsou, J.L. Yang, Chem. Biol. Interact. 102 (1996) 133–153.